A Shock Tube Study of Benzylamine Decomposition: Overall Rate Coefficient and Heat of Formation of the Benzyl Radical

Soonho Song, David M. Golden,* Ronald K. Hanson, and Craig T. Bowman

Department of Mechanical Engineering, Stanford University, Stanford, California 94305

Received: January 11, 2002; In Final Form: April 5, 2002

The decomposition rate of benzylamine ($C_6H_5CH_2NH_2$) and the heat of formation of the benzyl radical ($C_6H_5CH_2$) were determined in shock tube experiments combined with RRKM calculations. To obtain the decomposition rate of benzylamine, the NH_2 mole fraction was measured using frequency-modulation absorption spectroscopy behind reflected shock waves. The initial slope of the NH_2 concentration is directly proportional to the decomposition rate and the initial concentration of benzylamine. The rate expression for the decomposition reaction for the temperature range 1225−1599 K and the pressure range 1.19−1.47 bar is $k_1 = (5.49 \times 10^{14})e^{-33110/[T(K)]}$ s^{-1} with an uncertainty of ±15%. To obtain the high-pressure-limit rate expression for benzylamine decomposition, we performed RRKM calculations using the parameters obtained from the experimental data of this study and those of the VLPP study of Golden et al.[4] The resulting high-pressure-limit rate for the temperature range 1000−1600 K is $k_\infty = (1.07 \times 10^{16.0})e^{-36470/[T(K)]}$ s^{-1}. From the RRKM calculations, we determined the C−N bond dissociation energy of benzylamine at 0 K to be 305 ± 4 kJ mol^{-1}, and with this value and the thermochemical properties of benzylamine and NH_2, the heat of formation of the benzyl radical was calculated. The heat of formation of benzyl radical at 298 K is 210 ± 5 kJ mol^{-1}, which agrees with the result of Ellison et al.[5] and the value recommended by Tsang.[6]

Introduction

Benzylamine ($C_6H_5CH_2NH_2$) is an attractive source of NH_2 for shock tube kinetics experiments at temperatures as low as 1200 K, since benzylamine easily decomposes to produce NH_2 and the benzyl ($C_6H_5CH_2$) radical via reaction R1. This

$$C_6H_5CH_2NH_2 \rightarrow NH_2 + C_6H_5CH_2 \qquad \text{(R1)}$$

temperature corresponds approximately to the lower end of the shock tube operating conditions and the high-temperature limit of flow tube experiments. In addition, the benzyl radical is very stable and unlikely to react at such low temperatures.

In our previous shock tube study of the $NH_2 + NO$ reaction, we used benzylamine as a source of NH_2 for the temperature range 1262−1726 K and pressure range 1.14−1.44 bar.[1] To obtain the overall rate coefficient of this reaction, we needed to properly model the production of NH_2 from benzylamine pyrolysis. However, the decomposition rates determined in previous benzylamine pyrolysis studies[2−4] were not directly applicable for the temperatures and pressures of interest. For this reason, we measured the rate coefficient for benzylamine decomposition, k_1, for temperatures and pressures required in the $NH_2 + NO$ reaction study using the shock tube facility. To obtain k_1 values, we measured the concentration time history of the NH_2 radical produced from benzylamine pyrolysis using frequency modulation (FM) absorption and determined the decomposition rate of benzylamine by analyzing the initial rate of NH_2 production.

Another objective of this study is to determine the heat of formation of the benzyl radical. This value can be calculated from the bond dissociation energy, E_0, of the C−N bond of benzylamine at 0 K. Since E_0 is one of the input parameters for the RRKM calculation needed to evaluate the data, we used E_0 as a fitting parameter for the experimental data and obtained the value of E_0 compatible with the data.

Prior to this investigation, there have been several studies measuring the decomposition rate of benzylamine. Szwarc[2] used the toluene-carrier technique and determined the first-order reaction rate of benzylamine decomposition around 1000 K. Kerr and co-workers[3] also used the toluene-carrier flow technique to study pyrolysis of benzylamine for the temperature range of 830−1060 K. The results of a VLPP (very low pressure pyrolysis) study of benzylamine decomposition for the temperature range 1040−1250 K have been reported by Golden et al.[4] Since the unimolecular rate coefficient obtained from their VLPP experiment was in the falloff regime, they combined experimental data with the results of an RRKM calculation, using a model transition state, to determine the high-pressure-limit rate coefficient.

Recently, Ellison and co-workers reported the thermochemical properties of benzyl and allyl radicals.[5] In their experiments, they used a flowing afterglow/selected ion flow tube. Tsang has summarized the results of three different studies and/or reviews of the heat of formation of benzyl radical.[6] This included work by McMillen and Golden,[7] Hippler and Troe,[8] and Walker and Tsang.[9]

Experiments

The shock tube facility and diagnostics used in the present study were the same as those used in our previous study of the $NH_2 + NO$ reaction.[1] The NH_2 concentration was measured behind reflected shock waves using an FM absorption technique. With FM absorption, at least a factor of 10 reduction in the NH_2 detection limit can be achieved in comparison with direct laser absorption. The temperature and pressure behind the reflected shock wave were calculated from the initial temper-

10.1021/jp020085l CCC: $22.00
Published on Web 05/31/2002

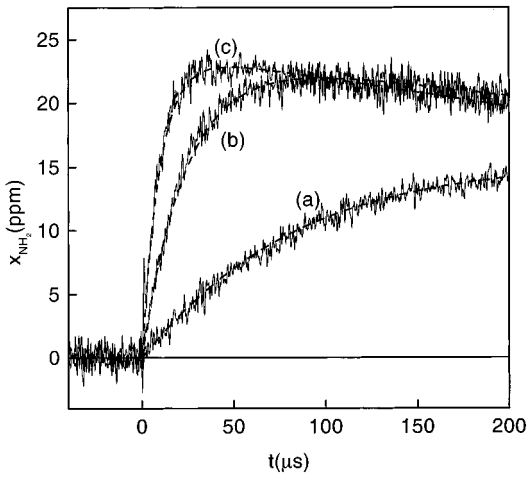

Figure 1. Example NH_2 mole fraction profiles: (a) 20 ppm $C_6H_5CH_2NH_2$/Ar balance, $T = 1309$ K, $P = 1.33$ bar; (b) 25 ppm $C_6H_5CH_2NH_2$/Ar balance, $T = 1410$ K, $P = 1.39$ bar; (c) 24 ppm $C_6H_5CH_2NH_2$/Ar balance, $T = 1489$ K, $P = 1.40$ bar. Solid lines are experimental data. Dashed lines are results of the CHEMKIN[21] calculations using the reaction mechanism reported in ref 1.

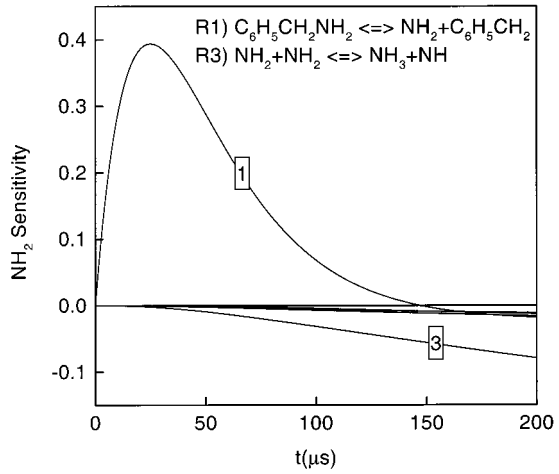

Figure 2. Result of SENKIN[22] calculation for NH_2 sensitivity using the reaction mechanism reported in ref 1: 25 ppm $C_6H_5CH_2NH_2$/Ar balance, $T = 1410$ K, $P = 1.39$ bar (conditions of Figure 1b).

ature and pressure and the shock speed measured over four intervals using five piezoelectric pressure gauges. The estimated uncertainty in the reflected shock temperature was less than ±20 K at 1400 K over the time intervals of interest.

Liquid benzylamine (>99.5%, Aldrich) was evaporated in a temperature-controlled bubble saturator, from which a mixture of Ar (>99.9999%, Praxair) and benzylamine vapor was continuously supplied to the shock tube. The flow scheme reduces the uncertainty in the initial concentration of benzylamine caused by wall adsorption. To measure the actual concentration of the benzylamine entering the shock tube, the absorption of benzylamine was measured between the bubble saturator and the shock tube using a 3.39 μm HeNe laser.

Experiments were performed in the temperature range 1225−1599 K, and the pressure range 1.19−1.47 bar. In total, 40 NH_2 traces were analyzed. The initial benzylamine concentration was varied from 20 to 50 ppm. Typical NH_2 traces are shown in Figure 1. When we analyzed the NH_2 traces, the initial slope of the NH_2 concentration was measured, and as can be seen from the sensitivity analysis in Figure 2, the initial slope is directly proportional to the decomposition rate of benzylamine and the initial concentration of benzylamine. The best fit rate

TABLE 1: Summary of k_1 with Experimental Conditions

T (K)	P (bar)	x_{BA} (ppm)	$k_1 \times 10^{-3}$ (s^{-1})	T (K)	P (bar)	x_{BA} (ppm)	$k_1 \times 10^{-3}$ (s^{-1})
1225	1.24	50	1.00	1405	1.41	25	28.0
1227	1.19	36	1.34	1405	1.41	25	36.7
1241	1.19	36	1.58	1410	1.39	25	44.0
1261	1.24	40	2.70	1431	1.42	25	67.0
1266	1.27	36	2.90	1432	1.35	25	50.0
1274	1.26	36	3.50	1434	1.40	25	62.0
1294	1.28	39	5.40	1453	1.47	26	73.0
1309	1.33	20	7.40	1468	1.39	29	97.0
1313	1.34	24	7.50	1475	1.39	28	103
1320	1.35	21	8.30	1486	1.22	23	141
1329	1.35	25	9.30	1488	1.37	30	125
1336	1.34	38	11.4	1489	1.40	25	130
1338	1.32	20	9.00	1496	1.37	28	150
1356	1.33	28	18.4	1498	1.43	28	137
1363	1.34	20	14.3	1499	1.33	27	160
1369	1.35	24	22.0	1541	1.26	20	270
1374	1.33	23	21.0	1544	1.32	29	280
1390	1.30	27	27.0	1573	1.39	26	420
1399	1.33	26	28.0	1598	1.30	31	647
1402	1.34	26	26.5	1599	1.36	23	610

expression for the pressure- and temperature-dependent value of k_1 for the experimental conditions of this study is

$$k_1/s^{-1} = 5.49 \times 10^{14} \exp[-33110/[T\,(K)]] (1225 < T\,(K) < 1599 \text{ and } 1.19 < P\,(\text{bar}) < 1.47) \quad (1)$$

The major sources of uncertainty are the uncertainty in the initial benzylamine concentration and the NH_2 absorption coefficient for the probe beam. The combined uncertainty is less than ±15%. Due to the direct measurement of the decomposition rate, the influence of secondary reactions is negligible. The measured rate coefficients and experimental conditions are tabulated in Table 1.

RRKM Calculation

RRKM calculations were performed to obtain the rate coefficient for benzylamine decomposition in the high-pressure limit and the bond dissociation energy of the C−N bond in benzylamine. To perform RRKM calculations. the structure and frequencies of the transition state are needed along with the critical energy and some knowledge of energy transfer. The structure and frequencies of the transition state yield the high-pressure A factor. If this is known, the critical energy can be used as a fitting parameter. In the earlier VLPP study of benzylamine,[4] Golden et al. used a simple fixed transition state. In this work, we treated the transition states using the "hindered-Gorin" model since a fixed transition state is an inadequate model for simple bond fission reactions.[10] With a fixed transition state, the heat capacity of the transition state is too high and the A factor for the dissociation reaction cannot be made compatible with the reverse recombination reaction when fixed vibrational frequencies are used for the low-frequency modes of the transition state. In the Gorin model, the internal modes of the transition state are the vibrations and rotations of the independent NH_2 and benzyl fragments. In other words, the transition state is treated as if NH_2 and benzyl radical were not covalently bonded but completely free to rotate. However, it has been noted that if the NH_2 and benzyl fragments were placed at a distance apart corresponding to the centrifugal maximum in a Lennard-Jones attractive potential, they would interact as they rotated, considering their van der Waals radii. Thus, the tightness of the transition state is characterized using the hindrance parameter, η, described by Smith and Golden,[10] as

TABLE 2: Inputs for the RRKM Calculations

$C_6H_5CH_2NH_2$ (Molecule)	
frequencies (cm^{-1})	3405, 3335, 3060, 3050, 3040, 3025, 3025, 2945, 2910, 1600, 1580, 1560, 1465, 1430, 1425, 1335, 1315, 1300, 1280, 1170, 1155, 1135, 1110, 1050, 1035, 1010, 975, 960, 935, 890, 875, 850, 820, 770, 735, 685, 610, 565, 475, 395, 350, 310, 245, 130, 45
product of adiabatic moments of inertia (10^{-80} g^2 cm^4)	4.022×10^5
Moment of inertia for active external rotor (10^{-40} g cm^2)	182.2
$C_6H_5CH_2\cdots NH_2$ (Transition State)	
frequencies (cm^{-1})	3305, 3230, 3115, 3065, 3055, 3050, 3040, 3035, 3025, 1530, 1515, 1495, 1445, 1440, 1420, 1305, 1270, 1235, 1140, 1130, 1075, 995, 960, 955, 940, 935, 865, 800, 745, 680, 660, 605, 515, 485, 460, 375, 345,190
product of adiabatic moments of inertia (10^{-80} g^2 cm^4)	9.097×10^5 at 1150 K 8.696×10^5 at 1400 K
moment of inertia for active external rotor (10^{-40} g cm^2)	253.5
moment of inertia for active 2-D rotor (10^{-40} g cm^2)	2.012 ($\sigma = 2$), 376.8 ($\sigma = 1$)
moment of inertia for active 1-D rotor (10^{-40} g cm^2)	2.145 ($\sigma = 3$)

TABLE 3: Data Used in Eq 4

species	T (K)	$\Delta_f H°$ (kJ mol^{-1})	uncertainty	ref
benzylamine	0	115.5	±2.7	23
NH_2	0	192	±1	24

the percentage of the 4π steradians unavailable to the rotating species. In effect, we are treating the rotations by varying the rotational level spacing through use of η, thereby controlling the entropy and heat capacity of the transition state. The hindrance is introduced into the RRKM code by multiplying the adiabatic two-dimensional rotor moments of inertia of the NH_2 and benzyl fragments in the transition state each by $(1 - \eta)^{1/2}$.

To analyze the shock tube data alone, employing the RRKM calculations, we had to estimate the high-pressure A factor, A_∞. The input parameters for the RRKM calculations cannot be determined by a single set of experimental data; therefore, either E_0 or A_∞ has to be estimated reasonably. We assumed that ethylbenzene ($C_6H_5CH_2CH_3$) decomposition chemistry was similar to that of benzylamine decomposition and used the A_∞ values of ethylbenzene for the RRKM calculations of benzylamine decomposition.

$$C_6H_5CH_2CH_3 \rightarrow CH_3 + C_6H_5CH_2 \qquad \text{(R2)}$$

According to Baulch et al.'s review,[11] the recommended A_∞ value for reaction R2 is 7.1×10^{15} s^{-1} for the temperature range 770−1800 K. Considering only papers published since 1980, the minimum[12] and maximum[13] values were 2.0×10^{15} and 1.3×10^{17} s^{-1}, respectively. We set the uncertainty of A_∞ as a factor of 4, and the corresponding range of A_∞ used for the RRKM calculations was from 1.6×10^{15} to 2.5×10^{16} s^{-1}. Within this range of A_∞, we calculated η and found the relationship between A_∞ and η at the mean temperature of the experimental conditions.

As stated earlier, RRKM calculations also require some knowledge of energy transfer. The simple pseudo-strong-collision version seems adequate for this study, which means knowing the value of the collision efficiency, β_c. Troe[14] has suggested that the collision efficiency, β_c, is related to the average energy transferred in a single collision, $\langle\Delta E\rangle_{all}$. Since the $\langle\Delta E\rangle_{all}$ value depends mostly on the bath gas (argon) rather than the reactant (benzylamine) and is a very weak function of T, we can estimate the range of $\langle\Delta E\rangle_{all}$ values of benzylamine−argon collisions even though experimental data are not available. The estimated $\langle\Delta E\rangle_{all}$ was -150 ± 50 cm^{-1}, which is similar to that in toluene−argon collisions.[15] After determining the $\langle\Delta E\rangle_{all}$ value and calculating β_c from a given $\langle\Delta E\rangle_{all}$, we obtained E_0 within uncertainty limits corresponding to the range of A_∞ values.

To reduce the uncertainty of the E_0 values, we needed to use (1) more accurate values of A_∞ or (2) other independent experimental data. To obtain the true value of A_∞, experiments should be performed at sufficiently high pressure. However, Brouwer and co-workers have reported that the ethylbenzene decomposition reaction (R2) was still in the falloff regime even at the highest experimental pressure,[13] which was 20 times higher than our experimental pressure. So instead, we reanalyzed the VLPP experimental data to obtain values of E_0 and A_∞ more accurately.

In contrast to the shock tube data analysis, where energy transfer is with gas−gas collisions, the efficiency of a gas−wall collision used in the VLPP, β_w, was required for the RRKM calculations. For some molecules, the β_w values were obtained experimentally, but data for benzylamine were not available, so we estimated the range of β_w values on the basis of a study by Dick et al.,[16] who pointed out that gas−wall collision under VLPP conditions had collision efficiencies of $\beta_w = 0.5 \pm 0.1$. In the VLPP study[4] performed prior to the work of Dick et al.,[16] a unit gas−wall collision efficiency ($\beta_w = 1$) was used. From the RRKM calculations with the given input parameters, we obtained combinations of A_∞ and E_0 fitting the VLPP as well as the shock tube data. The ranges of the $\langle\Delta E\rangle_{all}$ and β_w values automatically determine the uncertainty of the A_∞ and E_0 values.

In addition to the RRKM calculations, we used the Multiwell code,[17,18] which solves the master equation using a stochastic method. The average energy transfer used for deactivating collisions with argon, $\langle\Delta E\rangle_{down}$, was 550 cm^{-1} corresponding to $\langle\Delta E\rangle_{all} = -150$ cm^{-1}, and the results of the Multiwell calculation were consistent with those of the RRKM calculations.[19]

The frequencies and moments of inertia of the molecule and transition state were calculated using Gaussian 98, revision 7,[20] at the B3LYP/6-311G(d,p) level, and are tabulated in Table 3 with other input parameters for the RRKM calculation.

Results and Discussion

From the RRKM calculations, we determined the high-pressure-limit rate, k_∞, and the bond dissociation energy of the C−N bond of benzylamine at 0 K. Using the input parameters given in Table 3, the high-pressure rates were calculated every 100 K from 1000 to 1600 K. Fitting these rate coefficients linearly on an Arrhenius plot, we derived the rate expression

$$k_\infty/s^{-1} = 1.07 \times 10^{16} \exp[-36470/[T\,(K)]] \quad (1000\ K < T < 1600\ K) \qquad (2)$$

The A_∞ value given in eq 2 is 7 times the A_∞ value reported by Golden et al.[4] and 50% higher than the A factor for the ethylbenzene decomposition reaction recommended by Baulch et al.[11] The lower temperature limit of our experiments corre-

TABLE 4: Summary of Data on the High-Pressure-Limit Rate of Benzylamine Decomposition

authors (year)	methods (temperatures)	A_∞ (s^{-1})	E (kJ mol^{-1})	ref
Szwarc (1949)	toluene-carrier technique (920−1070 K)	6.0×10^{12}	247	2
Kerr et al. (1963)	toluene-carrier technique (830−1060 K)	1.0×10^{13}	250	3
Golden et al. (1972)	VLPP, RRKM (1040−1250 K)	1.58×10^{15}	301	4
Song et al. (2002)	shock tube, VLPP,[4] RRKM (1050−1600 K)	1.07×10^{16}	303	this study

TABLE 5: Summary of Data on the Benzyl Radical Heat of Formation

authors (year)	methods	$\Delta_f H°_{benzyl}$(300 K)	ref
McMillen and Golden (1982)	review	200 ± 6	7
Hippler and Troe (1990)	shock tube (pyrolysis of toluene, benzyl iodide, and dibenzyl)	210.5 ± 4	8
Walker and Tsang (1990)	shock tube (pyrolysis of *n*-pentylbenzene)	203 ± 6	9
Tsang (1996)	recommended value based on refs 7−9	207 ± 4	6
Ellison et al. (1996)	flowing afterglow/selected ion flow tube	208 ± 3	5
Song et al. (2002)	shock tube, VLPP[4]	210 ± 5	this study

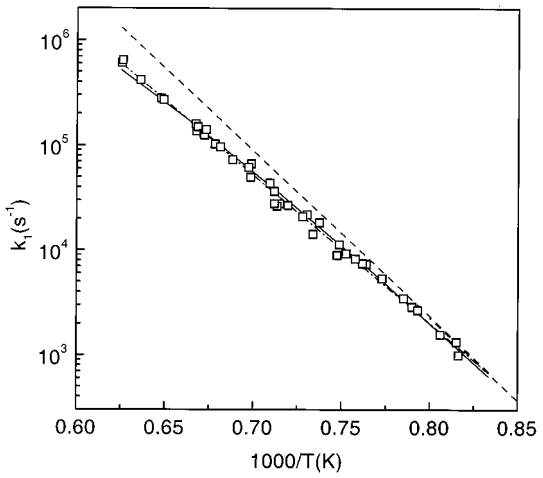

Figure 3. Shock tube experimental data for k_1: □, experimental data from this study ($P \approx 1.3$ bar); −•−, best fit to the experimental data near 1.3 bar, eq 1; solid line, results of the RRKM calculations at 1.3 bar; dashed line, results of the RRKM calculations for k_∞, eq 2.

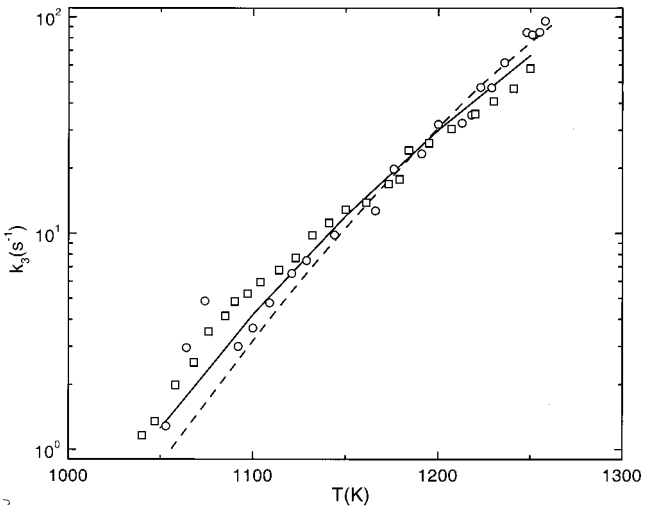

Figure 4. VLPP experimental data for k_1 taken from Table 3 and Figure 1 in ref 4: ○, VLPP experimental data (new reactor);[4] □, VLPP experimental data (old reactor);[4] dashed line, results of the RRKM calculations;[4] solid line, results of the RRKM calculations in this study.

sponds to the high-temperature limit of Szwarc's[2] and Kerr etal.'s[3] studies. At 1050 K, our k_∞ value is 2 times higher than that reported by Szwarc and 1.5 times higher than the value of Kerr et al. The extrapolated k_∞ values of eq 2 near 900 K agree with data from Szwarc and Kerr et al. within 20%. However, it is obvious that their A_∞ values ($\sim 10^{13}$ s^{-1}) are too low for the high-pressure-limit rate of the unimolecular decomposition reaction. The data from the shock tube experiments and the results of the RRKM calculation for k_1 (1.3 atm) and k_∞ are shown in Figure 3. The shock tube experimental conditions were in the falloff regime with k_1/k_∞ varying from 0.90 at 1200 K to 0.39 at 1600 K. The range of k_1/k_∞ was from 0.146 at 1050 K to 0.0292 at 1250 K for the VLPP experiments. The RRKM calculation for the VLPP data is shown in Figure 4.

Using only the shock tube data, we calculated the E_0 value as 297 ± 12 kJ mol^{-1}, but we were able to obtain a more accurate value by combining the shock tube and VLPP data. The resulting E_0 value was 305 ± 4 kJ mol^{-1}. The heat of formation of benzyl radical at 0 K, $\Delta_f H°_{benzyl}$(0 K), was calculated by eq 3, and the data are given in Table 5.

$$\Delta_f H°_{benzyl}(0\ K) = E_0 + \Delta_f H°_{benzylamine}(0\ K) - \Delta_f H°_{NH_2}(0\ K) = 228 \pm 5\ kJ\ mol^{-1} \quad (3)$$

To calculate the heat of formation of benzyl radical at 298 K, an appropriate heat capacity correction is required as shown in eq 4.

$$\Delta_f H°_{benzyl}(298\ K) = \Delta_f H°_{benzyl}(0\ K) - [H°(0\ K) - H°(298\ K)]_{benzyl} + 7[H°(0\ K) - H°(298\ K)]_C + 7/2[H°(0\ K) - H°(298\ K)]_{H2} \quad (4)$$

The sum of all correction terms is −18 kJ mol^{-1}, and the resulting value of $\Delta_f H°_{benzyl}$(298 K) was 210 ± 5 kJ mol^{-1}. This value is in good agreement with the result of Ellison et al.'s study,[5] 208 ± 3 kJ mol^{-1}, and Tsang's recommended value,[6] 207 ± 4 kJ mol^{-1}.

Table 4 summarizes values for the high-pressure-limit rate coefficient from past studies and the present study. Table 5 summarizes values for the heat of formation of benzyl radical.

Conclusions

We measured the benzylamine decomposition rate using frequency modulation absorption for NH_2 detection behind reflected shock waves in the temperature range 1225−1599 K around 1.3 bar. Combining the shock tube experimental data with earlier VLPP data, the high-pressure rate expression for benzylamine decomposition and the bond dissociation energy of the C−N bond of benzylamine were determined by applying RRKM calculations. The corresponding heat of formation of the benzyl radical was obtained from the bond dissociation

energy of the C−N bond of benzylamine and the thermochemical properties of benzylamine and NH_2.

Acknowledgment. This work was supported by the U.S. Department of Energy, Office of Basic Energy Sciences, Division of Chemical Sciences. We thank Juan Senosiain for performing the DFT calculations and John Barker for helpful discussions concerning use of the Multiwell code.

References and Notes

(1) Song, S.; Hanson, R. K.; Bowman, C. T.; Golden, D. M. *Int. J. Chem. Kinet.* **2001**, *33*, 715.
(2) Szwarc, M. *J. Chem. Phys.* **1949**, *17*, 505.
(3) Kerr, R. C.; Sekhar, R. C.; Trotman-Dickenson, A. F. *J. Chem. Soc.* **1963**, 3217.
(4) Golden, D. M.; Solly, R. K.; Gac, N. A.; Benson, S. W. *J. Am. Chem. Soc.* **1972**, *94*, 363.
(5) Ellison, G. B.; Davico, G. E.; Bierbaum, V. M.; DePuy, C. H. *Int. J. Mass Spectrom. Ion Processes* **1996**, *156*, 109.
(6) Tsang, W. In *Heats of Formation of Organic Free Radicals by Kinetic Methods in Energetics of Organic Free Radicals*; Martinho Simoes, J. A., Greenberg, A., Liebman, J. F., Eds.; Blackie Academic and Professional: London, 1996; pp 22−58.
(7) McMillen, D. F.; Golden, D. M. *Annu. Rev. Phys. Chem.* **1982**, *33*, 493.
(8) Hippler, H.; Troe, J. *J. Phys. Chem.* **1990**, *94*, 3803.
(9) Walker, J. A.; Tsang, W. *J. Phys. Chem.* **1990**, *94*, 3324.
(10) Smith, G. P.; Golden, D. M. *Int. J. Chem. Kinet.* **1978**, *10*, 489.
(11) Baulch, D. L.; Cobos, C. J.; Cox, R. A.; Esser, C.; Frank, P.; Just, Th.; Kerr, J. A.; Pilling, M. J.; Troe, J.; Walker, R. W.; Warnatz, J. *J. Phys. Chem. Ref. Data* **1992**, *21*, 411.
(12) Robaugh, D. A.; Stein, S. E. *Int. J. Chem. Kinet.* **1981**, *13*, 445.
(13) Brouwer, L.; Müller-Markgraf, W.; Troe, J. *Ber. Bunsen-Ges. Phys. Chem.* **1983**, *87*, 1031.
(14) (a) Troe, J. *J. Chem. Phys.* **1977**, *66*, 4745. (b) Troe, J. *J. Chem. Phys.* **1977**, *66*, 4758.
(15) Heymann, M.; Hippler, H.; Troe, J. *J. Chem. Phys.* **1984**, *80*, 1853.
(16) Dick, P. G.; Gilbert, R. G.; King, K. D. *Int. J. Chem. Kinet.* **1984**, *16*, 1129.
(17) Barker, J. R. Multiwell, 1.1.3 ed.; http://aoss.engin.umich.edu/multiwell/; Ann Arbor, MI, 2001.
(18) Barker, J. R. *Int. J. Chem. Kinet.* **2001**, *33*, 232.
(19) Barker, J. R.; Golden, R. E. *J. Chem. Phys.* **1984**, *88*, 1012.
(20) Frisch, M. J.; Trucks, G. W.; Schlegel, H. B.; Scuseria, G. E.; Robb, M. A.; Cheeseman, J. R.; Zakrzewski, V. G.; Montgomery, J.; Stratmann, R. E.; Burant, J. C.; Dapprich, S.; Millam, J. M.; Daniels, A. D.; Kudin, K. N.; Strain, M. C.; Farkas, O.; Tomasi, J.; Barone, V.; Cossi, M.; Cammi, R.; Mennucci, B.; Pomelli, C.; Adamo, C.; Clifford, S.; Ochterski, J.; Petersson, G. A.; Ayala, P. Y.; Cui, Q.; Morokuma, K.; Malick, D. K.; Rabuck, A. D.; Raghavachari, K.; Foresman, J. B.; Cioslowski, J.; Ortiz, J. V.; Baboul, A. G.; Stefanov, B. B.; Liu, G.; Liashenko, A.; Piskorz, P.; Komaromi, I.; Gomperts, R.; Martin, R. L.; Fox, D. J.; Keith, T.; Al-Laham, M. A.; Peng, C. Y.; Nanayakkara, A.; Gonzalez, C.; Challacombe, M.; Gill, P. M. W.; Johnson, B.; Chen, W.; Wong, M. W.; Andres, J. L.; Gonzalez, C.; Head-Gordon, M.; Replogle, E. S.; Pople, J. A. *Gaussian 98*, revision A.7; Gaussian Inc.: Pittsburgh, 1998.
(21) Lutz, A. E.; Kee, R. J.; Miller, J. A. *CHEMKIN-II: A Fortran Chemical Kinetics Package for the Analysis of Gas-Phase Chemical Kinetics*; Report SAND89-8009; Sandia National Laboratories: Albuquerque, NM, 1989.
(22) Lutz, A. E.; Kee, R. J.; Miller, J. A. *SENKIN: A Fortran Program for Predicting Homogeneous Gas Phase Chemical Kinetics with Sensitivity Analysis*; Report SAND87-8248; Sandia National Laboratories: Albuquerque, NM, 1987.
(23) Carson, A. S.; Laye, P. G.; Yurekli, M. *J. Chem. Thermodyn.* **1977**, *9*, 827.
(24) Anderson, W. R. *J. Phys. Chem.* **1989**, *93*, 530.